ELSEVIER

SCIENCE DIRECT

Physics Letters B 599 (2004) 190–196

PHYSICS LETTERS B

www.elsevier.com/locate/physletb

Antiproton stopping power in He in the energy range 1–900 keV and the Barkas effect

E. Lodi Rizzini [a], A. Bianconi [a], M.P. Bussa [a], M. Corradini [a], A. Donzella [a], M. Leali [a], L. Venturelli [a], N. Zurlo [a], M. Bargiotti [b], A. Bertin [b], M. Bruschi [b], M. Capponi [b], S. De Castro [b], R. Donà [b], L. Fabbri [b], P. Faccioli [b], B. Giacobbe [b], F. Grimaldi [b], I. Massa [b], M. Piccinini [b], N. Semprini Cesari [b], R. Spighi [b], S. Vecchi [b], M. Villa [b], A. Vitale [b], A. Zoccoli [b], O.E. Gorchakov [c], G.B. Pontecorvo [c], A.M. Rozhdestvensky [c], V.I. Tretyak [c], M. Poli [d], C. Guaraldo [e], C. Petrascu [e], F. Balestra [f], L. Busso [f], O.Y. Denisov [f,1], L. Ferrero [f], R. Garfagnini [f], A. Grasso [f], A. Maggiora [f], G. Piragino [f], F. Tosello [f], G. Zosi [f], G. Margagliotti [g], L. Santi [g], S. Tessaro [g]

[a] *Dipartimento di Chimica e Fisica per l'Ingegneria e per i Materiali, Università di Brescia and INFN, Gruppo Collegato di Brescia, Brescia, Italy*

[b] *Dipartimento di Fisica, Università di Bologna and INFN, Sezione di Bologna, Bologna, Italy*

[c] *Joint Institute for Nuclear Research, Dubna, Moscow, Russia*

[d] *Dipartimento di Energetica "Sergio Stecco", Università di Firenze, Firenze and INFN, Sezione di Bologna, Bologna, Italy*

[e] *Laboratori Nazionali di Frascati dell'INFN, Frascati, Italy*

[f] *Dipartimento di Fisica Generale "A. Avogadro", Università di Torino and INFN, Sezione di Torino, Torino, Italy*

[g] *Istituto di Fisica, Università di Trieste and INFN, Sezione di Trieste, Trieste, Italy*

Received 23 February 2004; accepted 16 August 2004

Available online 2 September 2004

Editor: M. Doser

Abstract

The $\bar{p}$ stopping power in helium from 1 keV kinetic energy is evaluated. Contrary to the effect observed around and below the maximum, Obelix data indicate a $\bar{p}$ stopping power higher than that for proton, the difference being of the order of $15 \pm 5\%$ at ≈ 700 keV. The result contributes to assert the fundamental difference between $\bar{p}$ stoppings in the simplest gases (He, H_2) and in solid targets below some MeV.

E-mail addresses: lodi@bs.infn.it (E. Lodi Rizzini), bussa@bs.infn.it (M.P. Bussa).

[1] On leave of absence from Joint Institute for Nuclear Research Dubna, Moscow, Russia.

0370-2693 © 2004 Elsevier B.V. Open access under CC BY license.
doi:10.1016/j.physletb.2004.08.040

1. Introduction

Atomic collisions have been studied during most of the past century. However, it is still a challenge to understand in detail even the simplest collision processes. This is due to the complex dynamics of systems that consist of more than two particles interacting via the Coulomb force.

At very high impact velocities the first Born approximation provides a convenient framework for the treatment of single ionization. On the contrary, for the double ionization process, the first Born approximation is not adequate, even at very high projectile velocities.

At a lower impact velocity, the target electronic cloud responds to the passage of the projectile by becoming polarized during the first part of the collision. This leads to a larger cross section for the proton than in the case of equivelocity antiproton impact. This difference grows when the velocity becomes smaller, but as the velocity approaches the magnitude of the orbital velocity, the polarization effect is counteracted by the so-called binding/antibinding effect [1]. Here close encounters become more important, and, as the projectile passes through the target electron cloud, the binding of the active electron is enhanced or reduced, depending on the sign of the projectile charge. This leads to a corresponding decrease or increase of the cross section.

Quinteros and Reading [2], Ermolaev [3,4], Frandsen et al. [5] and Lindhard [6] have discussed the possible interference and cancellation of these two effects and their possible observation in multi-electron systems [7].

Since the energy necessary for all processes comes from the projectile kinetic energy, measurement of the stopping cross section provides a consistency check for the individual cross sections.

A wide program of research was developed at the Low Energy Antiproton Ring (LEAR) at CERN to investigate the $\bar{p}$ stopping power around and below the maximum [8–12], both in solids and gaseous targets. New methods to measure stopping powers had to be worked out for these experiments, since the traditional methods used for protons and ions were not suited to exploit the properties of the antiproton projectile, in particular the annihilation process.

Moreover, the technique used for solid targets cannot be used for gaseous targets.

The main objective of these antiproton experiments was to determine the Barkas effect in the slowing down process, i.e., the difference in stopping power between positively and negatively charged particles.

A stopping power for $\bar{p}$ in various solid targets lower than the one for p by 35–55% has been measured in the low energy range of 1–100 keV at the new AD facility at CERN [13].

The measurements in solid targets represent a strong support for a velocity-proportional stopping power due to the target excitations by a point-like projectile as $\bar{p}$ (see also [14]).

On the contrary, the OBELIX experiment has measured striking departure from velocity-proportionality for $\bar{p}$ in gaseous H_2 and He [10,11] below the maximum contrary to the picture observed for p [15].

After a paper on the experimental result in gaseous H_2 [16], the simplest molecular system, in the work described in this Letter we evaluate the $\bar{p}$ stopping power in the range 1–900 keV in gaseous He, i.e., the simplest atomic system.

2. Data taking and analysis

The data used for the present study were collected by the Obelix experiment at LEAR with a helium target at the following pressures (at room temperature): 150, 50, 8.2 and 4 mbar. The uncertainty in the pressure values amounts to few percent. These samples were collected in the same experimental conditions as the hydrogen data [16]. A first analysis of these data is presented in [11].

Here we want to discuss the accuracy of the measurements in view of evaluation of the Barkas effect specifically above the maximum.

Unlike other experiments with solid targets based on the direct differential method (dE/dx), we derive the stopping power in a gaseous target by an integral method which combines the distribution of projectile ranges with the distribution of slowing down times for any antiproton. This method features high sensitivity to the energy losses of very slow projectiles.

The OBELIX apparatus is composed of a cylindrical 75 cm long gas target surrounded by a scintillator barrel and jet drift chambers to measure time and spatial coordinates of the vertex of an annihilation event inside the target within an accuracy of 1 ns and 1 cm,

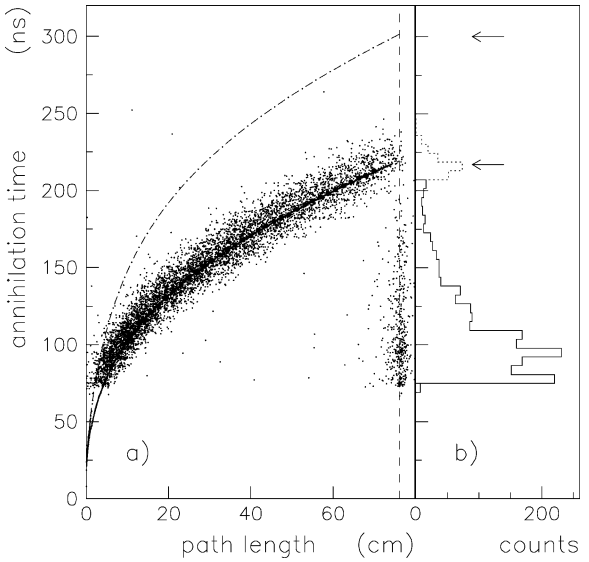

Fig. 1. (a) Scatter plot of the experimental $\bar{p}$ annihilation time versus path length at 50 mbar helium target pressure. Dots: mean values $(z_{\mathrm{exp}}, t_{\mathrm{exp}})$; full line: our best fit curve; dot-dashed line: curve derived from [14]. For the relevant parameters see text. (b) Full line: experimental $\bar{p}$ annihilation time at the end wall of the target vessel (dashed line in (a)). The dotted peak (lower arrow) corresponds to the contribution of the annihilations at rest in He for the two-centimeter bin preceding the end wall [17]; the corresponding time coming from the evaluation derived from [14] is indicated by the upper arrow.

respectively. Details of the apparatus and the measurement techniques can be found in [10–12].

The monochromatic $\bar{p}$ beam produced by the LEAR facility in the slow extraction mode (at the rate of a single $\bar{p}$ every microsecond) is suitably degraded in order to have a $\bar{p}$ energy continuously distributed from $E_i^{\min} \approx 0$ up to $E_i^{\max} \approx 1.1$ MeV at the entrance of the target. Therefore $\bar{p}$ annihilations are spread along the whole gaseous target at all the densities used, see Fig. 1a for the sample at 50 mbar.

Furthermore, it has to be observed that the annihilation-in-flight pattern, with a population not higher than 0.1%, is very different from that characteristic of annihilation at rest [18].

So, for each single $\bar{p}$ annihilation, the experiment gives information about the position along the beam z axis of the annihilation vertex at rest, together with the associated time t with respect to the start, indicated by a beam monitor scintillator, located just before the target.

For a better understanding of the power of our experimental method we notice that for each event the measured time is known with an accuracy of 1 ns, while the effective range of a $\bar{p}$ before capture at rest cannot be less than the measured z value. This means that in the scatter plot of Fig. 1a the annihilation vertex could be displaced to the right up to the boundary for that time. That is, the correction to the effective range can be no larger than the width of the experimental distribution at the measured time, which contains the straggling in the $\bar{p}$ energy loss, too. Therefore, the contours of the distribution in Fig. 1a determine the uncertainty in the stopping power $S(E)$ function [11].

This technique allowed to determine $S(E)$ at low $\bar{p}$ kinetic energies with a sensitivity that increases as the target density decreases [16].

In the (z,t) scatter plot of Fig. 1a we also present the mean values of the vertex z position and of the annihilation time $(z_{\mathrm{exp}}, t_{\mathrm{exp}})$ in each one of the two-centimeter-thick layers ideally subdividing the target fiducial volume along the z axis. The experimental annihilation time distributions for a 2 cm wide bin are different at any density but constant along the target. A typical distribution is reported in [10].

The mean values were fitted with a function $t = f(z)$ obtained by the simultaneous solution of both space $z_{\mathrm{exp}}(E)$ and time $t(E)$ integral relationships:

$$z_{\mathrm{exp}}(E_i) = \int_{E_{\mathrm{cap}}}^{E_i} \frac{dE}{S(E)}, \tag{1}$$

$$t(E_i) = \int_{E_{\mathrm{cap}}}^{E_i} \frac{dE}{vS(E)} = t_{\mathrm{exp}} - t_{\mathrm{cas}}. \tag{2}$$

The $\bar{p}$ laboratory kinetic energy E_i at the entrance of the target, the instantaneous velocity v and the $\bar{p}$ mean annihilation time t_{exp} all vary along the target. On the contrary, the $\bar{p}$ capture energy by the target atom, E_{cap}, and the mean cascade time t_{cas} of the $\bar{p}$–He system are constant along the target for each pressure [17].

Moreover, it is important to observe from (1) and (2) that t_{cas} is an additive constant, that can only shift the time of the expected annihilation vertex distributions up and down. Contrariwise, E_{cap} influences the shape of the annihilation distributions along the target, but the influence is lower the greater is E_i. The quantity t_{cas} is independently evaluated in our mea-

surements [17]. For E_{cap} we take into account the suggestion by Cohen [19]. We have determined the best E_{cap} value by χ^2 evaluation.

For the electronic stopping power $S(E)$ we have used, as for H_2, the interpolation formula $1/S = 1/S_l + 1/S_h$, where S_l (low energy stopping) $= \alpha E^{\beta}$ and S_h (high energy stopping) $= (484.5/E)\ln(1 + \gamma/E + 0.05225E)$ [20], where E is in keV, $S(E)$ is in eV 10^{-15} atoms^{-1} cm^2 and α, β, γ are free parameters. This way of extracting stopping powers is indirect and the results may in principle be dependent on the choice of the interpolation functions within the limits discussed in [11].

In Fig. 2a the electronic stopping power is presented, along with an acceptable behaviour for the nuclear stopping power (i.e., for the $\bar{p}$ interaction with the helium target nuclei below ≈ 1 keV). This nuclear stopping power behaviour comes out from the analysis of the data at lower pressures (0.2 and 1 mbar), as reported in Ref. [21].

The best fit to all the experimental values (z_{exp}, t_{exp}) at the different densities was obtained with the coefficients $\alpha = 1.45$, $\beta = 0.29$, $\gamma = 2.0 \times 10^5$, curve 1 in Fig. 2a [11], for the electronic stopping power. The total stopping power generates a $t = f(z)$ function that fits the data well at a 4 mbar pressure, the sample most sensitive to the nuclear stopping (see Fig. 3o).

The contribution above the maximum of the nuclear stopping power is small, as is the influence of E_{cap}.

In Fig. 1a we report the best fit $t = f(z)$ function, obtained from curve 1, superimposed on our experimental points, together with the behaviour expected if the stopping power proposed in [14] is taken into account. These authors reproduce successfully the data in solid targets and suggest a velocity-proportional behaviour from 1 keV up to the region of the maximum. We observe a striking disagreement in the case of gaseous helium. The $\bar{p}$ stopping function suggested in [14] presents a reduction by a factor of 3–4 in the energy region below and around the maximum, as compared to that of the proton. Moreover, it is observed in [13] that the $\bar{p}$ stopping power proposed in [14] around and below the maximum is clearly too low for carbon and aluminum.

Furthermore, in Fig. 1b we present the annihilation time distribution for $\bar{p}$ stopping in the end wall of the target (i.e., an independent time of flight measurement), whose initial kinetic energy is higher than

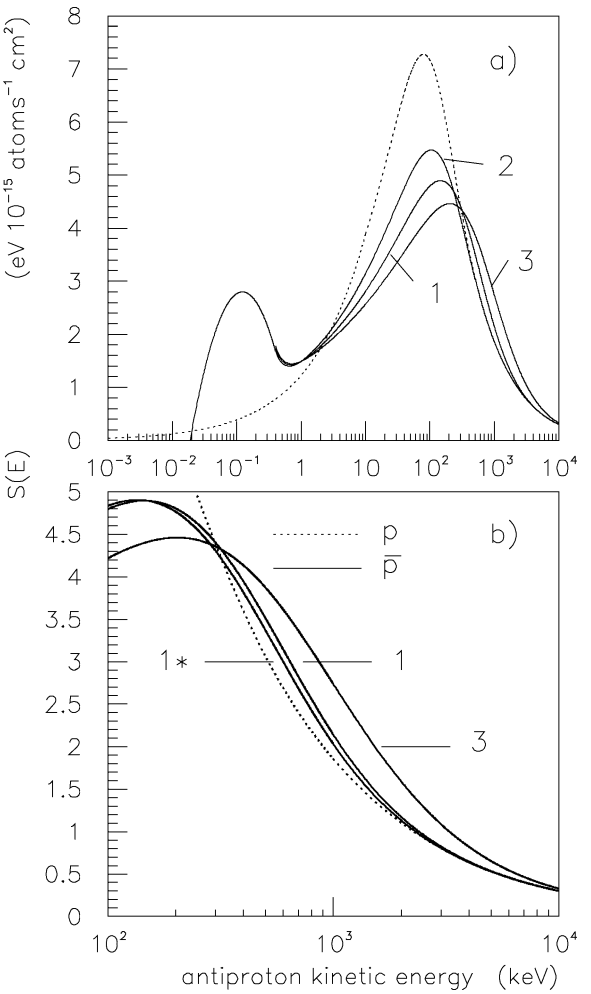

Fig. 2. (a) The best electronic $\bar{p}$ stopping power function in He (curve 1) above 1 keV, with two other analysed functions (curves 2 and 3). A $\bar{p}$ nuclear stopping power function for $\bar{p}$ energy below $\simeq 1$ keV is suggested. The proton behaviour is superimposed (dotted line); (b) enlargement of (a) in the region under the present analysis (for curve 1* see text).

that of $\bar{p}$ stopping just before the end wall. Again, it is evident from the very different position of the two arrows in Fig. 1b that the stopping function proposed in [14] fails to reproduce this time of flight distribution.

As we did for H_2, in Fig. 2a we compare the best stopping power function (curve 1) with two other functions, curves 2 and 3.

In Fig. 3, left column, the experimental points (z_{exp}, t_{exp}) and the $t = f(z)$ function produced from curve 1 for $E_{cap} = 25$ eV are shown for all pressure

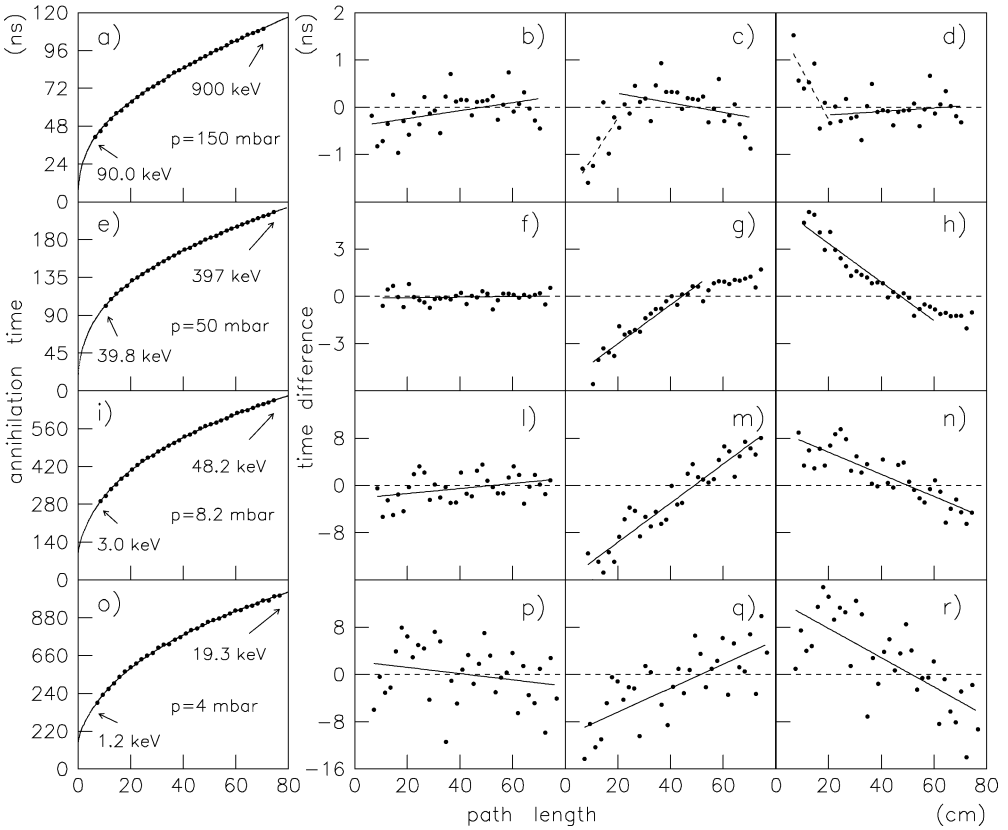

Fig. 3. Left column (a, e, i, o): mean $\bar{p}$ annihilation time versus path length at different He pressures and $E_{\text{cap}} = 25$ eV, with the best fitting curve 1. The arrows indicate the initial kinetic energy values E_i for the $\bar{p}$'s stopping in gas near the entrance and near the end wall of the target. Second column (b, f, l, p): time differences (ns) between experimental data and fitting curve with the interpolation straight line. Third (c, g, m, q) and fourth (d, h, n, r) columns: as second column for best fitting curves 2 and 3, respectively.

samples. In Fig. 3b, f, l, p the difference between the experimental and the best fit annihilation times of Fig. 3 (a, e, i, o left column) is shown, with an interpolating straight line to guide the eye. We see a good agreement between the experimental points and curve 1 (the slopes of the line are compatible with zero).

The last two columns of Fig. 3 contain the same information for curves 2 and 3, respectively. For the samples at 150 mbar (Fig. 3c, d) and 50 mbar pressure (Fig. 3g, h) the linear interpolation begins and ends, respectively, at ≈ 300 keV, where the $S(E)$ curve for $\bar{p}$ intersects that for p.

Fig. 3c, g, m, q shows quite an evident slope of the interpolating straight line up to ≈ 300 keV and show clearly that the slope of the $t = f(z)$ function related to curve 2 must be increased. This means that the function $S(E)$ should be lower in this range, according to (2). Therefore, a shift toward the left and a consequent enhancement of the $\bar{p}$ maximum (as in curve 2) are incompatible with the experimental data. We observe a different situation above ≈ 300 keV. This conclusion is quite evident from Fig. 3c, g. In Fig. 3c we see an inversion of the slope of the full line, with respect to the dashed line, and in Fig. 3g the points beyond the fit show a different behaviour, nearly horizontal. Moreover, for curve 3, Fig. 3d, h, n, r shows a drastic inversion in behaviour as compared with Fig. 3c, g, m, q. In general, Fig. 3, last column, suggests the necessity for curve 3 to rise until the $\bar{p}$ maximum and then to fall off.

To give a quantitative estimation of the Barkas effect in this energy region we show in Fig. 2b the proton curve, curves 1 and 3 and a new curve 1^*, very similar

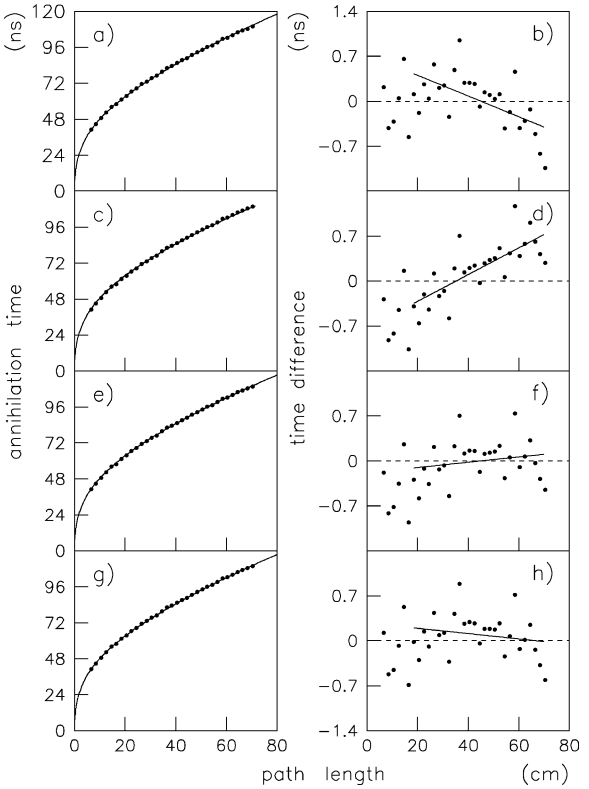

Fig. 4. Left column: mean $\bar{p}$ annihilation time versus path length at 150 mbar pressure and $E_{\mathrm{cap}} = 25$ eV, with the fitting curve $1+$proton (a), $1+3$ (c), 1 (e), $1+1^*$ (g). Right column: time differences (ns) between experimental data points and fitting curves with the interpolation straight line from $\simeq 300$ keV.

to curve 1 ($\alpha = 1.48$, $\beta = 0.29$, $\gamma = 1.2 \times 10^5$), that represents the best fit to the data in the region above the $\bar{p}$ maximum.

In Fig. 4a, c, e, g we present, only for the sample at 150 mbar, the experimental points $(z_{\mathrm{exp}}, t_{\mathrm{exp}})$ with the following $t = f(z)$ functions: curve 1 until 300 keV and then the proton curve (Fig. 4a) or curve 3 (Fig. 4c), curve 1 alone (Fig. 4e), curve 1 until the maximum (140 keV) and then curve 1^* (Fig. 4g). In Fig. 4b, d, f, h we show the difference between the experimental and the fitted annihilation times together with an interpolating straight line. The full lines in Fig. 4b, d have clearly opposite slopes, more accentuated in Fig. 4d. This fact indicates that the best $\bar{p}$ stopping power beyond the proton intersection is nearer to the proton stopping power than to curve 3. Anyway, the difference in the slopes tends to vanish in Fig. 4f, h.

So curve 1 and 1^* can be used to quantify the accuracy and sensitivity of our data for evaluating the $\bar{p}$ stopping power above the maximum.

Fig. 2b shows a maximum Barkas effect at ≈ 700 keV, with a difference in stopping power $S_{\bar{p}} - S_p$ of $15 \pm 5\%$. This is evaluated as the mean value between the ratios of curves 1^* and 1 for the antiproton and the proton curve ($\simeq 12\%$ and 18%, respectively), the error being the difference between curves 1 and 1^*. The difference $S_{\bar{p}} - S_p$ is nearly constant in the energy interval 600–800 keV, and tends to vanish beyond some MeV, like in the case of H_2.

3. Conclusions

Our results in He, together with our previous result in H_2, show that the behaviour of $\bar{p}$ stopping in gases is very different with respect to that in solid targets. Below its maximum, the $\bar{p}$ stopping power does not exhibit a velocity—proportionality and above the maximum the difference $\bar{p} - p$ is even positive, as suggested by some theoretical predictions.

On the contrary, theoretical models for the $\bar{p}$ stopping power based on free-electron-gas description of the stopping medium seem to be inadequate for the simplest atoms and molecules like He and H_2.

In conclusion, He stopping powers below some MeV both for p and $\bar{p}$ result to be a very interesting and fundamental subject for the understanding of Coulomb interactions in few body systems.

References

[1] G. Schiwietz, U. Wille, R. Diez Muino, P.D. Fainstein, P.L. Grande, J. Phys. B 29 (1996) 307.
[2] T.B. Quinteros, J.F. Reading, Nucl. Instrum. Methods B 53 (1991) 363.
[3] A.M. Ermolaev, Phys. Lett. A 149 (1990) 151.
[4] A.M. Ermolaev, J. Phys. B 23 (1990) 45.
[5] N.P. Frandsen, et al., XVIII I.C.P.E.A.C. Abstract of Contributed Papers, vol. II, Aarhus Univ. Press, Aarhus, 1993, p. 397.
[6] J. Lindhard, Nucl. Instrum. Methods 132 (1976) 1.
[7] J.F. Reading, In atomic hydrogen with only one electron the effect is evaluated very small or completely absent, private communication, 2002.
[8] S.P. Møller, Nucl. Instrum. Methods B 48 (1990) 1.
[9] R. Medenwaldt, et al., Phys. Lett. A 155 (1991) 155.
[10] A. Adamo, et al., Phys. Rev. A 47 (1993) 4517.

[11] M. Agnello, et al., Phys. Rev. Lett. 74 (1995) 371.
[12] A. Bertin, et al., Phys. Rev. A 54 (1996) 5441.
[13] S.P. Møller, A. Csete, T. Ichioka, H. Knudsen, U.I. Uggerhøj, H.H. Andersen, Phys. Rev. Lett. 88 (2002) 193201.
[14] P. Sigmund, A. Schinner, Eur. Phys. J. D (2001) 165.
[15] A. Schiefermüller, R. Golser, R. Stohl, D. Semrad, Phys. Rev. A 48 (1993) 4467.
[16] E. Lodi Rizzini, et al., Phys. Rev. Lett. 89 (2002) 183201.
[17] A. Bianconi, et al., Phys. Lett. B 487 (2000) 224.
[18] A. Zenoni, et al., Nucl. Instrum. Methods A 447 (2000) 512.
[19] J.S. Cohen, Phys. Rev. A 62 (2000) 0225121.
[20] C. Varelas, J.P. Biersack, Nucl. Instrum. Methods 79 (1970) 213.
[21] A. Bianconi, et al., Phys. Rev. A, submitted for publication.